Forebrain engraftment by human glial progenitor cells enhances synaptic plasticity and learning in adult mice

Xiaoning Han[1,2], **Michael Chen**[1,2], **Fushun Wang**[1,2], **Martha Windrem**[1,3], **Su Wang**[1,3], **Steven Shanz**[1,3], **Qiwu Xu**[1,2], **Nancy Ann Oberheim**[1,2], **Lane Bekar**[1,2], **Sarah Betstadt**[4], **Alcino J. Silva**[5], **Takahiro Takano**[1,2], **Steven A. Goldman**[1,2,3,*], and **Maiken Nedergaard**[1,2,3,*]

[1]Center for Translational Neuromedicine, University of Rochester Medical Center, Rochester, NY, 14642 USA

[2]Dept. of Neurology, University of Rochester Medical Center, Rochester, NY, 14642 USA

[3]Dept. of Neurosurgery, University of Rochester Medical Center, Rochester, NY, 14642 USA

[4]Dept. of Obstetrics and Gynecology, University of Rochester Medical Center, Rochester, NY, 14642 USA

[5]Depts. of Neurobiology, Psychiatry and Psychology, Integrative Center for Learning and Memory, UCLA David Geffen School of Medicine, Los Angeles, CA 90095 USA

Abstract

Human astrocytes are larger and more complex than those of infraprimate mammals, suggesting that their role in neural processing has expanded with evolution. To assess the cell-autonomous and species-selective properties of human glia, we engrafted human glial progenitor cells (GPCs) into neonatal immunodeficient mice. Upon maturation, the recipient brains exhibited large numbers and high proportions of both human glial progenitors and astrocytes. The engrafted human glia were gap junction-coupled to host astroglia, yet retained the size and pleomorphism of hominid astroglia, and propagated Ca^{2+} signals 3-fold faster than their hosts. Long term potentiation (LTP) was sharply enhanced in the human glial chimeric mice, as was their learning, as assessed by Barnes maze navigation, object-location memory, and both contextual and tone fear conditioning. Mice allografted with murine GPCs showed no enhancement of either LTP or learning. These findings indicate that human glia differentially enhance both activity-dependent plasticity and learning in mice.

Keywords

glial progenitor cell; chimera; astrocyte; long-term potentiation; learning

*Address correspondence to either: Steve Goldman, M.D., Ph.D., Center for Translational Neuromedicine, University of Rochester Medical Center, 601 Elmwood Rd., Box 645, Rochester, NY 14642, Steven_Goldman@urmc.rochester.edu, Phone: 585-275-9550, Maiken Nedergaard, M.D., Ph.D., Center for Translational Neuromedicine, University of Rochester Medical Center, 601 Elmwood Rd., Box 645, Rochester, NY 14642, nedergaard@urmc.rochester.edu, Phone: 585-275-9550, Fax: 585-276-2298.

INTRODUCTION

The unique processing capabilities of the human brain reflect a number of evolutionary adaptations by its cellular constituents (Fields, 2004). One especially distinct feature of the adult human brain's cellular composition is the size and complexity of its astrocytic cohort. Human astrocytes are both morphologically and functionally distinct from those of infraprimate mammals, in that human astroglia are larger, and exhibit far greater architectural complexity and cellular pleomorphism, as well as more rapid syncytial calcium signaling, than their murine counterparts (Colombo, 1996; Oberheim et al., 2009). These phylogenetic differences are of particular interest, since astrocytes can both coordinate and modulate neural signal transmission (Rusakov et al., 2011; Verkhratsky et al., 1998). These observations promise to fundamentally transform our view of astrocytes, since current concepts of the role of astrocytes in neural network performance are based almost entirely on studies of astrocytic physiology in the rodent brain (Oberheim et al., 2006).

In this study, we have used a novel human glial-chimeric mouse brain to ask whether the structural complexity and unique functional properties of human astrocytes influence activity-dependent plasticity in an otherwise stable neural network. In particular, we have tested the hypothesis that human astrocytes might enhance synaptic plasticity and learning, relative to their murine counterparts.

RESULTS

Human glial progenitors exhibit cell-autonomous astrocytic differentiation in mouse brain

To study human astrocytes in the live adult brain, we generated chimeric mice in which human glial progenitor cells (GPCs) - isolated by sorting on the basis of an A2B5$^+$/PSA-NCAM$^-$ phenotype, and then expanded using a protocol that promoted differentiation into hGFAP and A2B5 expressing astrocytes (Fig. S1A) - were xenografted into neonatal immune-deficient mice; these matured to become adults chimeric for both mouse and human astroglia (Windrem et al., 2004; Windrem et al., 2008). (Fig.1A). The human GPCs were labeled ex vivo, prior to implantation, with VSVg-pseudotyped lentiviral-CMV-EGFP; in antecedent pilot experiments, we had determined that this vector sustained the expression of EGFP by astroglial for at least a year in vivo (Fig. 1A). The neonatally-implanted mice were sacrificed at time-points ranging from 0.5-20 months of age, and their brains assessed both histologically and electrophysiologically. Human donor cells were first identified based on their expression of human nuclear antigen (hNuclei). The hNuclei+ cells were found to distribute relatively evenly throughout the forebrain, infiltrating both hippocampus and cortex (Fig. 1B). Human astrocytes were specifically identified by their intricate EGFP$^+$ fluorescent processes, and in fixed tissue by their co-expression of human glial fibrillary acidic protein (hGFAP) and hNuclei (Fig. 1C). By 4-5 months of age, mice engrafted with human GPCs exhibited substantial addition of human astrocytes to both the hippocampus and deep neocortical layers; by 12-20 months, human astrocytes further populated large regions of the amygdala, thalamus, neostriatum and cortex (Fig. 1D-F). The human astrocytes appeared to develop and mature in a cell-autonomous fashion, maintaining their larger size and more complex structure relative to murine astrocytes (Fig. 1G-H).

Human astrocytes, defined as EGFP$^+$/hGFAP$^+$/hNuclei$^+$, regularly extended processes that terminated in end-feet contiguously arrayed along blood vessel wall (Fig. 2A-B). Their long processes were often tortuous, and resembled the processes of interlaminar astroglia, a phenotype previously described only in adult human and ape brain (Oberheim et al., 2006) (Fig. 2C); these cells are characterized by long, unbranched processes that traverse multiple cortical laminae (Colombo, 2001). Many of the engrafted human astrocytes in chimeric mice extended processes that spanned >0.5 mm (Fig. 2D). A large number of mitochondria were

present in the long processes (Fig. 2E). Other engrafted human cells exhibited the long, varicosity-studded processes of varicose projection astrocytes, a second class of hominid astrocytes (Oberheim et al., 2009).

Of note, rag2$^{-/-}$ immunodeficient mice on a C3h background were generally used as recipients for these experiments, although rag1$^{-/-}$ immunodeficient mice (on a C57/Bl6 background) were used for vision-dependent behavioral tests, since the C3h background of the rag2 mice is a visually impaired strain; we observed no difference in xenograft acceptance, cell dispersal or differentiation patterns between these two hosts. In that regard, we found no evidence of microglial activation in the xenografted mice, whether in rag1- or rag2-null hosts, reflecting both their neonatal engraftment and immunodeficient backgrounds (Figs. S1B-F)

Human astrocytes coupled structurally and functionally with mouse astrocytes

Their cell-autonomous maturation and morphologies notwithstanding, the engrafted human cells rapidly integrated with murine host cells. The gap junction tracer Alexa 594 (MW 760), once injected into EGFP$^+$ human cells, spread rapidly into multiple neighboring EGFP$^-$ host cells, suggesting the competence of interspecies gap junctions linking human and mouse astroglia, likely derived from the apposition of human and mouse connexin 43 hemi-channels (Fig. 2F). A large number of hNuclei$^+$ cells failed to express GFAP, but did express a human specific isoform of the chondroitin sulfate proteoglycan, NG2 (Fig. 2G), a prototypic marker of parenchymal glial progenitor cells (Mangin and Gallo, 2011; Robel et al., 2011). Of note, hGFAP$^+$ and hNG2$^+$ human cells often co-existed in close proximity, although their relative ratios exhibited considerable variation across regions, as well as between individual mice (Fig. 2G). Transferrin immunostaining failed to detect any human oligodendroglia, consistent with our prior assessment of glial progenitor cell fate upon transplantation to normally-myelinated brain (Windrem et al., 2009) (Figs. S2A-B): Whereas a large proportion of engrafted human GPCs differentiate into oligodendrocytes in hypomyelinated shiverer mice, essentially no human oligodendrocytes were found in similarly engrafted wild-type mice (Windrem et al., 2009).

Human GPCs and astrocytes exhibited distinct physiological phenotypes in mouse brain

To evaluate the electrophysiological properties of human astrocytes engrafted in mice, acute hippocampal slices were prepared from chimeric mice ranging from 4-10 months of age (6.5 ± 0.4 months–old, mean ± SD). Donor astrocytes could be readily identified by their EGFP fluorescence, and by their large, symmetric, highly branched astrocytic morphologies. The tagged donor cells were filled with Alexa 594 or the Ca^{2+} indicator rhod2 during whole-cell recordings, and their phenotype verified by immunolabeling for GFAP (Fig. 3A). EGFP$^+$ human astrocytes exhibited a higher input resistance than that of host murine astrocytes (51.6 ± 2.5 MΩ, n=37, vs. 29.2 ± 3.2 MΩ, n=17, respectively, means ± SEM; p<0.05, Steel-Dwass test). In contrast, the resting membrane potential of human astrocytes (-69.2 ± 1.5mV, n=37) was not significantly different from that of untagged host astrocytes (-73.9 ± 1.7 mV; n=17; p>0.05) (Figs. 3B-D). Whereas all large and symmetric EGFP$^+$ donor cells exhibited passive membrane currents and linear current to voltage (I/V) curves, another population of smaller EGFP$^+$ human cells with compact, asymmetrically branched morphologies manifested a much higher input resistance (147.8 ± 11.7MΩ, n=14). These donor cells manifested voltage-gated currents and depolarization-triggered outward currents with delayed activation (Fig. 3B), and expressed a human epitope of chondroitin sulfate proteoglycan NG2, identifying them as persistent glial progenitors (Fig. 2G) (Kang et al., 2010; Robel et al., 2011). Together, these histological and electrophysiological analyses supported the notion that a large proportion of engrafted human cells differentiated into

protoplasmic astrocytes, forming a functional syncytium with their murine host, and that these were accompanied by large numbers of co-engrafted $NG2^+$ human glial progenitors.

Human astrocytes propagate calcium waves more quickly than do murine astroglia

Astrocytes are electrically non-excitable, and are incapable of electrochemical communication. Instead, the principle mechanism of astrocytic signaling involves transient elevations of cytosolic Ca^{2+} (Cotrina and Nedergaard, 2005). In light of the larger and more complex architecture of human astrocytes, we next asked whether propagation of intracellular Ca^{2+} signals in human astrocytes differs from that of rodents. To compare intracellular Ca^{2+} wave propagation between human and mouse astrocytes, we initiated localized Ca^{2+} increases by photolysis of caged Ca^{2+} (Parpura and Verkhratsky, 2011; Rusakov et al., 2011). Photolysis of caged Ca^{2} loaded specifically into astrocytes was used to avoid potentially confounding alterations in local synaptic activity. Intracellular Ca^{2+} waves were evoked by directing a UV beam at long processes of astrocytes filled with rhod-2 and NP-EGTA by a patch pipette. The subsequent spread of Ca^{2+} signals was visualized using 2-photon excitation (Fig. 3E). Line scanning with high temporal resolution (2-4 ms) showed that intracellular Ca^{2+} wave propagation was significantly faster in human astrocytes than murine cells; intracellular Ca^{2+} increases propagated with a velocity of 15.8 $\pm$ 0.7 µm/s among human glia, compared to 5.7 $\pm$ 0.4 µm/s in resident murine astrocytes (n=22-34, 6.5 $\pm$ 0.4 vs. 7.0 $\pm$ 0.5 months-old, mean $\pm$ SEM; p<0.05, Steel-Dwass test) (Fig. 3F-H). To determine whether the faster intracellular Ca^{2+} waves in human astrocytes were an artifact of xenograft, we also assessed intracellular Ca^{2+} wave spread in slices of fresh human brain tissue, obtained at surgical resection for distant lesions (mean age of patients: 30.6 $\pm$ 8.8 years, n = 3). Human astrocytes in these surgical resections similarly propagated intracellular Ca^{2+} waves much more rapidly than did murine astrocytes (n=10) (Fig. 3H). Together, these experiments demonstrated that intracellular Ca^{2+} signals propagate at least 3-fold faster within human astrocytes than in their rodent counterparts, and do so in human glial chimeric mice just as in human brain tissue. Of note, we were unable to evaluate intercellular Ca^{2+} wave propagation, as only slices prepared from young mice pups load well with esterified (AM) Ca^{2+} indicators (Dawitz et al., 2011).

Human astrocytes accentuate excitatory synaptic transmission in the murine hippocampus

A principal function of astrocytes is to monitor local synaptic activity by their expression of metabotropic neurotransmitter receptors for both glutamate and GABA (Parpura and Verkhratsky, 2011; Rusakov et al., 2011). These receptors activate intracellular signaling pathways, mediated primarily by increases in cytosolic Ca^{2+}, which are linked to synaptic plasticity (Parpura and Zorec, 2010). To assess the selective impact of human astrocytes on neural transmission within the host murine neural network, we compared synaptic activity in hippocampal slices prepared from human glial chimeric mice, to that of both their unengrafted and allografted littermate controls. We focused on the hippocampal dentate granule layer, because of the many electrophysiological and behavioral tests by which hippocampal function, learning and LTP could be assessed (Lee and Silva, 2009). In addition, human cells typically densely engrafted this area; these included an admixture of $GFAP^+/hNuclei^+$ and $NG2^+/hNuclei^+$ cells (Figs. 1B, F, 2G). Stimulation of the medial perforant path (Colino and Malenka, 1993) consistently evoked a significantly steeper slope of field excitatory postsynaptic potentials (fEPSP) in the humanized chimeric mice than in either their uninjected littermates or mouse GPC allografted controls (n=3-40; F=3.15, by two-way ANOVA; p=0.044) (Fig. 4A). The allograft controls comprised a set of mice neonatally engrafted with murine GPCs derived from EGFP transgenic mice, otherwise using the same isolation and engraftment protocols as those using human GPCs. The steeper slope of the fEPSPs in the humanized chimeras compared to uninjected controls was still

evident after normalization to the fiber volley amplitudes, a measure thought to reflect the number of stimulated axons (Fig. S3A). Thus, slices with human glia exhibited a significant enhancement in their basal level of excitatory synaptic transmission, over a wide range of stimulation intensities.

Human astrocytes enhance LTP in the adult murine hippocampus

We next asked if human astrocytes might affect synaptic plasticity, by assessing the effect of human glia on long-term potentiation (LTP). Two trains of high frequency stimulation (HFS) potentiated the fEPSP slope to $151.2 \pm 8.1\%$ of baseline in chimeric mice, compared with $138.6 \pm 7.6\%$ in control littermates (n = 7 mice in both groups; 13.8 ± 1.1 vs. 12.6 ± 0.4 months-old, respectively; ages provided as mean $\pm$ SEM) (Fig. 4B). The enhancement of fEPSP slope persisted at 60 min in humanized chimeric mice (113.6 ± 3.8 %, p < 0.05), whereas fEPSP slope in unengrafted controls fell to 103.2 ± 3.9 % (not significantly different from the fEPSP slope prior to HFS; p=0.169). Mouse allografted controls exhibited an initial increase to $138.5 \pm 2.3\%$, which fell to 103.8 ± 1.3 % at 60 min (not significantly different from the fEPSP slope prior to HFS; n = 7, 14.0 ± 0.1 months-old; p = 0.29, t test) (Fig. 4B). Thus, the observed enhancement of LTP was a specific feature of human glial chimerization, and were not attributable to cell engraftment per se.

The enhancement of LTP can result from both pre- and post-synaptic mechanisms. An analysis of paired-pulse facilitation before and after high frequency stimulation in chimeric mice suggested that post-synaptic mechanisms most likely underlie the enhancement of fEPSP slope in humanized chimeric mice (Figs. S3B-C). To evaluate the relative contribution of AMPA and NMDA receptor-mediated currents to the enhancement in LTP in the chimeric mice, we analyzed the effect of NMDA receptor blockade, using the NMDA receptor antagonist APV. We found that the NMDA receptor component accounted for only 4.7-12% of fEPSP, with no significant differences across the groups analyzed, indicating that NMDA NR1 expression was not increased in the human glial chimeras. These findings suggest that NMDA receptor activation played a minor role, if any, in the enhancement of synaptic plasticity in the chimeric mice (n=15-27) (Fig. 4C). Since NMDA receptors have a higher affinity for glutamate than do AMPA receptors (Malinow and Malenka, 2002), these observations also suggest that the potentiation of fEPSPs in human glial chimeric mice was not the result of increased synaptic release of glutamate; this is consistent with the lack of enhancement of paired-pulse suppression in the chimeric mice (Fig. S3B-C).

Neither adenosine nor D-serine accounted for the enhancement of LTP by human glia

Several mechanisms exist by which astrocytes can modulate excitatory transmission. Astrocytes release ATP, which after degradation to adenosine by extracellular ectonucleotidases, can suppress both basal synaptic transmission, and activity-dependent increases in synaptic strength (Pascual et al., 2005; Zhang et al., 2003). However, it seems unlikely that adenosine contributed to the enhanced synaptic strength observed in the xenografted mice. The A1 receptor antagonist, 8-cyclopentyl-1,3-dipropylxanthine (DPCPX) (Grover and Teyler, 1993; Wu and Saggau, 1994) did not decrease the threshold for induction of LTP in control mice; in slices exposed to 100 nM DPCPX, the fEPSP slope returned to $101.9 \pm 3.6\%$ 60 min after HFS, similar to untreated slices (Figs. 4D-E). Thus, it is unlikely that the reduced threshold for LTP in chimeric mice was a consequence of altered adenosine concentrations.

Astrocytes can also modulate excitatory transmission via their release of D-serine (Panatier et al., 2006; Yang et al., 2003). D-serine acts as an endogenous co-agonist of NMDA receptors and facilitates NMDA receptor activation, thereby potentiating the insertion of additional AMPA receptors into the post-synaptic membrane (Panatier et al., 2006; Yang et

al., 2003). We tested the effect of adding D-serine to the bath of slices prepared from control mice. D-serine had no effects on the fEPSP slopes in accordance with previous reports (p=0.216, n=6) (Panatier et al., 2006; Yang et al., 2003). Moreover, neither D-serine nor immunolabeling for its synthetic enzyme, serine racemase, differed between human glial chimeric and uninjected control mice (Fig. S3D-E). These observations suggest that the lower threshold for induction of LTP in human glial chimerics was not a consequence of altered adenosine tone or increased glial release of D-serine.

Human glial TNFα potentiates synaptic transmission via an increase in GluR1 receptors

Release of the cytokine TNFα comprises an alternative mechanism by which glia might modulate LTP. Cultured astrocytes constitutively release TNFα, which induce the addition of AMPA receptors to neuronal membranes, thereby enhancing excitatory synaptic transmission (Beattie et al., 2002; Stellwagen and Malenka, 2006). To assess the involvement of TNFα in the strengthening of excitatory transmission in the human glial chimeric mice, we first confirmed that TNFα increased both AMPA receptor current (Fig. 5A) and AMPA GluR1 immunolabeling in hippocampal slices (Fig. 5B). In contrast, TNFα did not affect expression of the NMDA receptor NR1 subunit in the same slices (Fig. 5B). On that basis, we next asked whether chimeric mice expressed human TNFα. Using qPCR we found that human-specific sequence encoding TNFα was indeed highly expressed in the chimeras, yet undetectable in unengrafted mice (Fig. S4A). Immunolabeling confirmed that the human glial chimeras exhibited significant increases in both TNFα and GluR1, but not of NR1 (Fig. 5C). We thus asked whether the inhibition of TNFα production might suppress excitatory hippocampal transmission in chimeric mice, and if so, whether TNFα inhibition might abrogate the effects of human glial chimerization on LTP.

Previous studies have analyzed the effect of TNFα on excitatory transmission in vitro, by adding soluble TNFR1 receptors to scavenge free TNFα (Beattie et al., 2002; Stellwagen and Malenka, 2006). Since soluble TNFR1 would not be expected to be an efficient inhibitor in vivo, we instead administered thalidomide, a potent, BBB permeable inhibitor of TNFα production (Ryu and McLarnon, 2008). Human glial chimeric mice treated with thalidomide exhibited a significant suppression of fEPSP slopes compared to those receiving vehicle (0.5% carboxy-methylcellulose) (1.41 ± 0.15 mV/ms vs. 1.05 ± 0.24 mV/ms at 0.1mA; means ± SEM; p<0.05, n = 12). In contrast, excitatory transmission in unengrafted littermates was unaffected by thalidomide (1.02 ± 0.12 mV/ms vs. 0.97 ± 0.20 mV/ms at 0.1mA; p=0.32, n =12). These observations suggested that thalidomide selectively targeted the potentiation of excitatory transmission mediated by human glial TNFα. Accordingly, thalidomide also reduced the expression of both TNFα and GluR1 in the human glial chimeras, but not that of NR1 (Fig. 5D). Importantly, thalidomide also prevented the facilitation of LTP in the human glial chimeras: Two trains of HFS failed to trigger LTP in slices taken from chimeras pre-treated with thalidomide (106.3 ± 3.9%, n=6, 12.6 ± 0.3 months of age), whereas the activity-dependent potentiation of fEPSPs persisted in vehicle-treated human glial chimeras (117.6 ± 4.8 %, n=6, 12.5 ± 0.5 months; p<0.05, t test) (Fig. 5E). Thalidomide did not alter the number of NMDA receptors activated in response to medial perforant-path fiber stimulation in either chimeric or unengrafted controls, suggesting that thalidomide specifically suppressed the number of functional AMPA receptors consistent with prior publications showing that TNFα drives membrane insertion of AMPA receptors (Fig. 5F) (Beattie et al., 2002; Stellwagen and Malenka, 2006). Thus, TNFα released by human glial cells (Fig. S4A, Fig. 5C) enhanced host neuronal fEPSPs by increasing the number of functional postsynaptic GluR1 AMPA receptors (Fig. 5C), and conversely, thalidomide suppressed plasma membrane insertion of AMPA, but not NMDA receptors by inhibiting TNFα production (Fig. 5D).

TNFα regulates a number of cellular processes through protein kinase C (PKC)-mediated phosphorylation (Faurschou and Gniadecki, 2008), which is thus disrupted by thalidomide. Since phosphorylation of GluR1, at sites critical for its synaptic delivery, is both necessary and sufficient for lowering the threshold for inducing LTP (Hu et al., 2007), we thus next asked if the phosphorylation state of the GluR1 subunit differed between human glial chimeric mice and their littermate controls. We focused on two phosphorylation sites, Ser845 (PKA site) and Ser831 (PKC/CaMKII site), each of which is critical for the synaptic insertion of GluR1 (Hu et al., 2007), and assessed the effects upon each of human glial chimerization, and of thalidomide. Quantitative immunohistochemistry revealed that human glial chimeric mice exhibited a significant increase in Ser831 phosphorylation, the PKC-sensitive site (n=6; p=0.008, t-test); this was significantly attenuated in human glial chimeras receiving thalidomide, but not in their unengrafted control littermates (n=9-10; p>0.4, t test) (Fig. 5G). In contrast, phosphorylation of the Ser845 PKA site was unaffected by either the engraftment of human glia, or by thalidomide (n=6, p > 0.05, t test) (Fig. S4B-C). Together, these results suggested that human glia facilitate synaptic insertion of the GluR1 subunit in host murine neurons, through a TNFα-dependent, PKC/CamKII-mediated pathway, which lowers the threshold for induction of LTP in human glial chimeric mice.

Enhanced learning in humanized chimeric mice

Stable, long-lasting changes in synaptic function, such as those revealed by our LTP studies, are thought to be involved in learning and memory (Lee and Silva, 2009). Since LTP was markedly enhanced in human glial chimeric mice, we next asked if these mice also exhibited improved learning. We first assessed whether auditory fear conditioning (AFC) - a task in which the mice learn to fear an innocuous tone by pairing it with foot shock (Zhou et al., 2009), and which does not require visual input (rag2$^{-/-}$ mice are blind; Chang et al., 2007) - was potentiated in the human glial chimeras. To this end, we compared the rate of acquisition of AFC by xenografted human glial chimeras to that of both allografted murine glial chimeras, and unengrafted littermate controls (Fig. 6A). The allografted mice – which were also generated in immunodeficient rag2-null hosts - received neonatal grafts of A2B5^{+}/PSA-NCAM^{-} cells isolated from transgenic mice with constitutive EGFP expression, allowing the ready identification of murine donor cells. After just a single pairing of the tone with foot shock, the human glial chimeric mice exhibited a significant enhancement in learning of the tone foot shock association: They showed greater fear to the tone as measured by scoring freezing behavior (the cessation of all movement except for respiration), than did either allografted chimeras or unengrafted controls (n = 5-20; 9.6 ± 1.0 months-old; F = 18.9, two-way repeated measures ANOVA; p < 0.001). Moreover, after 3 continuous days of training humanized chimeric mice also showed enhanced AFC during the 3 remaining days of testing, as manifested by their higher levels of freezing in response to the conditioned tone (p<0.01, post hoc Bonferroni test). In contrast, neither murine glial chimeric mice nor unengrafted controls manifested any increase in freezing behavior during the same period, despite having been subjected to an identical fear conditioning paradigm (p>0.05; Bonferroni test) (Fig. 6A). Of note, no differences were observed in the reaction to foot shock between the human glial chimeras and their controls (n=5, 9.6 ± 1.0 months old; F = 0.08 by two-way ANOVA, p>0.5) (Fig. S5A), suggesting that their respective nociceptive thresholds were analogous.

To specifically assess hippocampus-dependent learning, we next prepared chimeric mice using rag1 immunodeficient mice (maintained on a C57/Bl6 background), which differ from their rag2-null counterparts (on a C3H background) by having normal vision. We first compared the net engraftment of human GPCs, as well as their relative differentiation into hNG2^{+} GPCs or GFAP+ astroglia, in human glial chimeras established in rag1-null and rag2-null mice. We focused on hippocampal learning, as this region was used for our

analysis of LTP (Lee and Silva, 2009; Manns and Eichenbaum, 2009). We found that both the engraftment and differentiation of human GPCs in rag1- and rag2-immunodeficient mice were indistinguishable from one another (Fig. S5B-C). On that basis, we next assessed the effect of chimerization of rag1-null immunodeficient mice on contextual fear conditioning (CFC), a hippocampal-dependent task in which mice learn to fear a context in which they receive a foot shock (Fanselow and Poulos, 2005). The human glial-chimeric mice exhibited enhanced performance in CFC throughout all 4 days of training (Fig. 6B). By just the second day, the human glial-chimeric mice exhibited substantially more rapid and robust CFC than their non-chimeric littermate controls (n=6; 6.9 ± 0.1 months of age; F = 14.8 by two-way repeated measures ANOVA, p=0.003), and continued to display enhanced CFC during the subsequent 2 days of CFC training (Fig. 6B). To exclude the possibility that a generalized increase in freezing behavior could explain the observed differences, we also examined the context-specificity of freezing responses. In these experiments, the mice were placed in a second chamber with a different floor and odor. Chimeric mice exhibited superior discrimination between the two contexts, suggesting stronger contextual learning, as opposed to a non-specific higher level of fear (n=8-13; 7.6 ± 0.1 months; p<0.05, t-test) (Fig. 6B). No differences were observed in the reaction times to foot shock between the human glial chimeras and their rag 1-null immunodeficient controls (n=5, 9.6 ± 0.95 month, F = 0.08 by two-way ANOVA, p>0.5) (Fig. S5A). Moreover, neither thermal nor mechanical sensitivity were affected by chimerization of either rag1 or rag2 mice (Figs. S5D-E), suggesting that their respective nociceptive thresholds were analogous.

To better assess the scope of performance enhancement in the human glial chimeras, we next assessed their performance in the Barnes maze, another hippocampal-dependent learning task. In this spatial learning task mice learn the location of a hole that leads to an escape/drop box. By just the second day of serial daily testing, the human glial chimeras made fewer errors and displayed a significantly shorter latency in finding the drop box, compared to their littermate controls (n=6, 7.4 ± 0.1 months; F=13.4 by two-way repeated measures ANOVA, p=0.004) (Fig. 6C). These differences persisted throughout the four-trial testing period (n=6, 7.4 ± 0.1 months; F=11.4, p=0.007). With additional training, the unengrafted control mice were capable of completing the task, indicating that they could master the task if given sufficient training (Fig. S5F).

Next, we tested the mice in the Object-Location Memory Task (OLT), another hippocampal dependent task (Manns and Eichenbaum, 2009). OLT tests the ability of the animal to recognize a familiar object in a novel location. Chimeric mice exhibited a substantially greater preference for objects in novel locations than their controls (58.6 ± 4.8% vs. 41.8 ± 2.3%, means ± SEM; n=7, 7.2 ± 0.1 months, p = 0.008, t-test) (Fig. 6D). Thalidomide treatment did not affect appreciably the performance of the unengrafted littermate controls on the OLT, but reduced the performance of the human glial chimeric mice to the levels of controls (n=7, 7.8 ± 0.1 months, p=0.82, t test) (Fig. 6D). Thus, thalidomide selectively abrogated the chimerization-associated performance enhancement of the human glial chimeras.

Together, these results indicate that relative to either unengrafted mice or mice allografted with A2B5[+]/PSA-NCAM[-]-sorted, EGFP[+] murine GPCs, human glial-chimeric mice exhibit enhanced performance in 4 different learning tasks: auditory and contextual fear conditioning, Barnes maze, and novel object-location. Moreover, the analysis of auditory fear conditioning indicate that alloengraftment by mouse GPCs did not affect the learning of the recipient mice, supporting the notion that the improved learning in the humanized chimeras resulted from the presence of human glia, rather than from cell engraftment per se. As an additional control, we also noted that social interactions did not differ between human chimeras generated by engraftment in rag1 mice and their littermate controls (n=5, 6.9 ± 0.1

months; p>0.05, t test) (Figs. S5G-H), indicating that chimerization did not seen to affect their interactions with other mice.

DISCUSSION

Prior studies have documented that astrocytes regulate synaptic transmission, and actively participate in the synaptic efficiency of neural circuits in the rodent CNS (Fields, 2004; Nedergaard and Verkhratsky, 2012; Parpura and Verkhratsky, 2011; Rusakov et al., 2011). A parallel, hitherto non-overlapping line of work has shown that human astrocytes are larger and far more structurally complex than those of rodents (Colombo, 1996; Oberheim et al., 2009); this has led to the hypothesis that astrocytic evolution has been critical to the increased scope and capacity of central neural processing that have attended hominid evolution (Colombo, 1996; Oberheim et al., 2012; Oberheim et al., 2006). In support of this hypothesis, genomic studies have revealed that the greatest differences in brain gene expression between humans and mice are in glial transcripts (Miller et al., 2010).

In this study, we created human glial-chimeric mice, in which immunodeficient but otherwise normal mice were engrafted neonatally with large numbers of human glial progenitors, resulting in the widespread integration of human glia into the mouse brain. By the time these mice reached adulthood, a large proportion of their forebrain glia were replaced by human cells. The chimerization was slowly progressive, so that extensive infiltration of cortex and hippocampus by human cells was evident by 4-12 months (Fig. 1). The xenografted human cells remained as NG2-defined glial progenitor cells or differentiated as hGFAP$^+$ astrocytes; remarkably, the latter maintained their characteristic, large and complex hominid-selective morphologies (Fig. 2). In addition, some assumed the characteristic long-distance fiber extensions of interlaminar astrocytes, a domain-traversing astrocytic phenotype specific to the hominid brain (Colombo, 2001; Colombo et al., 1995; Oberheim et al., 2006). Electrophysiological analysis validated that most EGFP$^+$/hGFAP$^+$/hNuclei$^+$ human glia were protoplasmic astrocytes, based on their low input resistance, passive membrane properties, extensive gap junction coupling, and Ca^{2+} wave propagation (Fig. 3).

The striking population of the recipient mouse brains by human glia raised the possibility that the engrafted human cells might significantly modulate information processing within the host murine neural networks. Indeed, the basal level of excitatory synaptic transmission was increased over a wide range of stimulation intensities. The presence of human glia also enhanced long-term potentiation in human glial-chimeric hippocampal slices, relative to mice that had received conspecific murine glial progenitors or vehicle injection (Fig. 4). Our analysis showed that TNFα was significantly elevated in the human glial chimeric brains, consistent with the potentiation of AMPA receptor-mediated currents (Beattie et al., 2002; Stellwagen and Malenka, 2006). Additional analysis suggested that TNFα may have directly facilitated insertion of the GluR1 subunit to the plasma membrane (Hu et al., 2007), perhaps via its increased phosphorylation at Ser831. TNFα might also potentiate astrocytic glutamate release (Ni and Parpura, 2009; Parpura and Zorec, 2010), which in turn could increase GluR1 subunit phosphorylation by NMDA receptor-mediated activation of PKC (Fig. 5) (Malinow and Malenka, 2002). These pathways might both have contributed to the enhancement of hippocampal LTP that we observed in the human glial chimeras, although we found no evidence of enhancement of NMDA receptor activation after engraftment (Fig. 4C). Importantly, we found that thalidomide, a BBB-permeable inhibitor of TNFα, both diminished the enhancement of post-synaptic AMPA receptor current and reduced LTP in chimeric mice, yet had no such effects in unengrafted littermate controls. Behavioral analyses then revealed that human glial-chimeric mice exhibited improved learning and memory in four different tasks, including auditory and contextual fear conditioning, the

Barnes Maze, and Object-Location Memory Task (Fig. 6). As with the chimerization-associated enhancement in LTP, the enhanced learning of chimeric mice in the object location recognition assay was eliminated by thalidomide treatment (Fig. 6D). Engraftment by neonatally delivered mouse GPCs enhanced neither LTP nor either auditory fear conditioning or Barnes maze performance, strongly suggesting that the potentiation of synaptic plasticity and learning afforded by glial progenitor cell chimerization was specific to human glia, and not a product of cell engraftment per se (Figs. 4B, 6A).

Together, these studies demonstrate that human astrocytes generated within the mouse brain maintain their complex phenotype in a cell-autonomous fashion; they assume morphologies and Ca^{2+} wave characteristics typical of the human brain, but hitherto never observed in experimental animals. These observations strongly support the notion that the evolution of human neural processing, and hence the species-specific aspects of human cognition, in part may reflect the course of astrocytic evolution (Oberheim et al., 2006). As such, these human glial-chimeric mice may present a fundamentally new experimental model by which human glial cells, and both normative and pathological species-specific aspects of human glial biology, may now be effectively studied in the live adult brain.

EXPERIMENTAL PROCEDURES

Isolation of human and murine glial progenitor cells

Fetal glial cells progenitors were extracted from 17 to 22-week-old human fetuses obtained at abortion. The forebrain ventricular and subventricular zones were dissected free on ice and then were dissociated using papain/DNAase as described (Windrem et al., 2004). All samples were obtained with consent under approved protocols of the University of Rochester Research Subjects Review Board. Glial progenitor cells were isolated by magnetic activated cell sorting, as described in Supplementary Methods. In addition, murine A2B5[+]/PSA-NCAM^{-} cells were identically prepared from newborn Tg(CAG-EGFP)B5Nagy/J pups (Jackson Laboratory).

Transfection and differentiation

A2B5[+]/PSA-NCAM^{-} cells were transfected to express enhanced EGFP, as described in the Supplementary Methods.

Transplantation

Human glial chimeras were prepared as described, using either rag1-/- or rag2-/- immunodeficient mice (as described in Windrem et al., 2008, though using mice wild-type for myelin); see Supplementary Methods for additional detail. All experiments were approved by the University of Rochester's Research Animal Care and Use Committee.

Quantitative immunohistochemistry

Chimeric mice and littermate controls (ranging from 2 weeks - 20 months, depending upon experimental endpoint) were perfusion-fixed, processed histologically and analyzed as described in Supplementary Methods.

Electrophysiological characterization of human glia in chimeric mice

Patch clamp assessment of engrafted human glia was performed in slice preparations, under two-photon microscopy, as detailed in Supplementary Methods.

Long term potentiation

Slice preparations of both chimeric mice and their littermate controls (age range 7–20 months) were used for recordings of field excitatory postsynaptic potentials (fEPSPs), as well as for analyzing activity-dependent changes in hippocampal synaptic strength, as outlined in Supplementary Methods.

Ca^{2+} Imaging and photolysis of caged Ca^{2+}

Chimeric mice (age range 4-10 months) were used for imaging intracellular Ca^{2+} in xenografted human glia. In addition, as positive controls, surgical resections of human cortex (n=3 patients; 30.6 ± 8.8 years-old) were obtained with patient consent and the approval of the University of Rochester Research Subjects Review Board; all samples were prepared for physiological assessment and analyzed as described in Supplementary Methods.

Detection of human TNFα in human glial chimeras

RNA isolation, PCR primer design, reverse transcription, and PCR reaction conditions and analysis are all described in Supplementary Methods.

Learning tasks and behavioral assessment

Auditory fear conditioning, contextual conditioning, Barnes maze navigation, object location memory, Crawley's social interaction tasks, and both thermal and mechanical sensitivity thresholds were assessed in human glial chimeric and control mice; the latter included allografted and/or unengrafted negative controls. All tests and analyses were performed as outlined in Supplementary Methods.

Statistics

All data are presented and graphed as means $\pm$ SEM. The Steel-Dwass test was used to assess the relative diameters of cells, input resistances, and Ca^{2+} velocities, all variables for which normality of the data could not be assumed. For other electrophysiological data, either Student's t-test for two groups, or two-way ANOVA with Bonferroni post hoc t-tests, were used. For behavioral data, Student's t test or two-way repeated measures ANOVA with Bonferroni post hoc test were used. Normality of the data was assessed by the Shapiro-Wilk test. P values <0.05 were considered significant.

Supplementary Material

Refer to Web version on PubMed Central for supplementary material.

Acknowledgments

References

Beattie EC, Stellwagen D, Morishita W, Bresnahan JC, Ha BK, Von Zastrow M, Beattie MS, Malenka RC. Control of synaptic strength by glial TNFalpha. Science. 2002; 295:2282–2285. [PubMed: 11910117]

Colino A, Malenka RC. Mechanisms underlying induction of long-term potentiation in rat medial and lateral perforant paths in vitro. Journal of neurophysiology. 1993; 69:1150–1159. [PubMed: 8492154]

Colombo AJ. A columnar-supporting mode of astroglial architecture in the cerebral cortex of adult primates? Neurobiology (Bp). 2001; 9:1–16. [PubMed: 11558929]

Colombo JA. Interlaminar astroglial processes in the cerebral cortex of adult monkeys but not of adult rats. Acta Anat (Basel). 1996; 155:57–62. [PubMed: 8811116]

Colombo JA, Yanez A, Puissant V, Lipina S. Long, interlaminar astroglial cell processes in the cortex of adult monkeys. J Neurosci Res. 1995; 40:551–556. [PubMed: 7616615]

Cotrina, M.; Nedergaard, M. Intracellular calcium control mechanisms in glia. 2. New York: Oxford University Press; 2005.

Dawitz J, Kroon T, Hjorth JJ, Meredith RM. Functional calcium imaging in developing cortical networks. Journal of visualized experiments : JoVE. 2011

Fanselow MS, Poulos AM. The neuroscience of mammalian associative learning. Annu Rev Psychol. 2005; 56:207–234. [PubMed: 15709934]

Faurschou A, Gniadecki R. TNF-alpha stimulates Akt by a distinct aPKC-dependent pathway in premalignant keratinocytes. Exp Dermatol. 2008; 17:992–997. [PubMed: 18557926]

Fields RD. The other half of the brain. Scientific American. 2004; 290:54–61. [PubMed: 15045754]

Grover LM, Teyler TJ. Role of adenosine in heterosynaptic, posttetanic depression in area CA1 of hippocampus. Neurosci Lett. 1993; 154:39–42. [PubMed: 8395668]

Hu H, Real E, Takamiya K, Kang MG, Ledoux J, Huganir RL, Malinow R. Emotion enhances learning via norepinephrine regulation of AMPA-receptor trafficking. Cell. 2007; 131:160–173. [PubMed: 17923095]

Kang SH, Fukaya M, Yang JK, Rothstein JD, Bergles DE. NG2+ CNS glial progenitors remain committed to the oligodendrocyte lineage in postnatal life and following neurodegeneration. Neuron. 2010; 68:668–681. [PubMed: 21092857]

Lee Y-S, Silva A. The molecular and cellular biology of enhanced cognition Nat Rev Neurosci. 2009; 10:126–140.

Malinow R, Malenka RC. AMPA receptor trafficking and synaptic plasticity. Annual review of neuroscience. 2002; 25:103–126.

Mangin JM, Gallo V. The curious case of NG2 cells: transient trend or game changer? ASN neuro. 2011; 3:e00052. [PubMed: 21288204]

Manns JR, Eichenbaum H. A cognitive map for object memory in the hippocampus. Learn Mem. 2009; 16:616–624. [PubMed: 19794187]

Miller JA, Horvath S, Geschwind DH. Divergence of human and mouse brain transcriptome highlights Alzheimer disease pathways. Proc Natl Acad Sci U S A. 2010; 107:12698–12703. [PubMed: 20616000]

Nedergaard M, Verkhratsky A. Artifact versus reality-How astrocytes contribute to synaptic events. Glia. 2012; 60:1013–1023. [PubMed: 22228580]

Ni Y, Parpura V. Dual regulation of Ca2+-dependent glutamate release from astrocytes: vesicular glutamate transporters and cytosolic glutamate levels. Glia. 2009; 57:1296–1305. [PubMed: 19191347]

Oberheim NA, Goldman SA, Nedergaard M. Heterogeneity of astrocytic form and function. Methods in molecular biology. 2012; 814:23–45. [PubMed: 22144298]

Oberheim NA, Takano T, Han X, He W, Lin JH, Wang F, Xu Q, Wyatt JD, Pilcher W, Ojemann JG, et al. Uniquely hominid features of adult human astrocytes. J Neurosci. 2009; 29:3276–3287. [PubMed: 19279265]

Oberheim NA, Wang X, Goldman S, Nedergaard M. Astrocytic complexity distinguishes the human brain. Trends Neurosci. 2006; 29:547–553. [PubMed: 16938356]

Panatier A, Theodosis DT, Mothet JP, Touquet B, Pollegioni L, Poulain DA, Oliet SH. Glia-derived D-serine controls NMDA receptor activity and synaptic memory. Cell. 2006; 125:775–784. [PubMed: 16713567]

Parpura V, Verkhratsky A. The astrocyte excitability brief: From receptors to gliotransmission. Neurochem Int. 2011

Parpura V, Zorec R. Gliotransmission: Exocytotic release from astrocytes. Brain Res Rev. 2010; 63:83–92. [PubMed: 19948188]

Pascual O, Casper KB, Kubera C, Zhang J, Revilla-Sanchez R, Sul JY, Takano H, Moss SJ, McCarthy K, Haydon PG. Astrocytic purinergic signaling coordinates synaptic networks. Science. 2005; 310:113–116. [PubMed: 16210541]

Robel S, Berninger B, Gotz M. The stem cell potential of glia: lessons from reactive gliosis. Nature reviews Neuroscience. 2011; 12:88–104.

Rusakov DA, Zheng K, Henneberger C. Astrocytes as regulators of synaptic function: a quest for the Ca2+ master key. The Neuroscientist : a review journal bringing neurobiology, neurology and psychiatry. 2011; 17:513–523.

Ryu JK, McLarnon JG. Thalidomide inhibition of perturbed vasculature and glial-derived tumor necrosis factor-alpha in an animal model of inflamed Alzheimer's disease brain. Neurobiol Dis. 2008; 29:254–266. [PubMed: 17964176]

Stellwagen D, Malenka RC. Synaptic scaling mediated by glial TNF-alpha. Nature. 2006; 440:1054–1059. [PubMed: 16547515]

Verkhratsky A, Orkand RK, Kettenmann H. Glial calcium: homeostasis and signaling function. Physiol Rev. 1998; 78:99–141. [PubMed: 9457170]

Windrem, MS.; Moyle, C.; Chandler-Militello, D.; Han, X.; Nedergaard, M.; Wang, S.; Goldman, S. Program No 12621/A48 Neuroscience Meeting Planner. Chicago, IL: Society for Neuroscience Online; 2009. Neonatally-implanted human glial progenitor cells out-compete endogenous glial progenitor cells to generate fully humanized glial-chimeric mouse brains.

Windrem MS, Nunes MC, Rashbaum WK, Schwartz TH, Goodman RA, McKhann G 2nd, Roy NS, Goldman SA. Fetal and adult human oligodendrocyte progenitor cell isolates myelinate the congenitally dysmyelinated brain. Nat Med. 2004; 10:93–97. [PubMed: 14702638]

Windrem MS, Schanz SJ, Guo M, Tian GF, Washco V, Stanwood N, Rasband M, Roy NS, Nedergaard M, Havton LA, et al. Neonatal chimerization with human glial progenitor cells can both remyelinate and rescue the otherwise lethally hypomyelinated shiverer mouse. Cell Stem Cell. 2008; 2:553–565. [PubMed: 18522848]

Wu LG, Saggau P. Adenosine inhibits evoked synaptic transmission primarily by reducing presynaptic calcium influx in area CA1 of hippocampus. Neuron. 1994; 12:1139–1148. [PubMed: 8185949]

Yang Y, Ge W, Chen Y, Zhang Z, Shen W, Wu C, Poo M, Duan S. Contribution of astrocytes to hippocampal long-term potentiation through release of D-serine. Proc Natl Acad Sci U S A. 2003; 100:15194–15199. [PubMed: 14638938]

Zhang JM, Wang HK, Ye CQ, Ge W, Chen Y, Jiang ZL, Wu CP, Poo MM, Duan S. ATP released by astrocytes mediates glutamatergic activity-dependent heterosynaptic suppression. Neuron. 2003; 40:971–982. [PubMed: 14659095]

Zhou Y, Won J, Karlsson MG, Zhou M, Rogerson T, Balaji J, Neve R, Poirazi P, Silva AJ. CREB regulates excitability and the allocation of memory to subsets of neurons in the amygdala. Nature neuroscience. 2009; 12:1438–1443.

Highlights

- Neonatal implantation of human glial progenitors generates glial chimeric brains

- Hominid-specific astrocytic properties are retained in a cell-autonomous fashion

- Human glial chimerization enhances TNFα–dependent long-term potentiation

- Human glial chimeric mice are faster learners across a range of behavioral tests
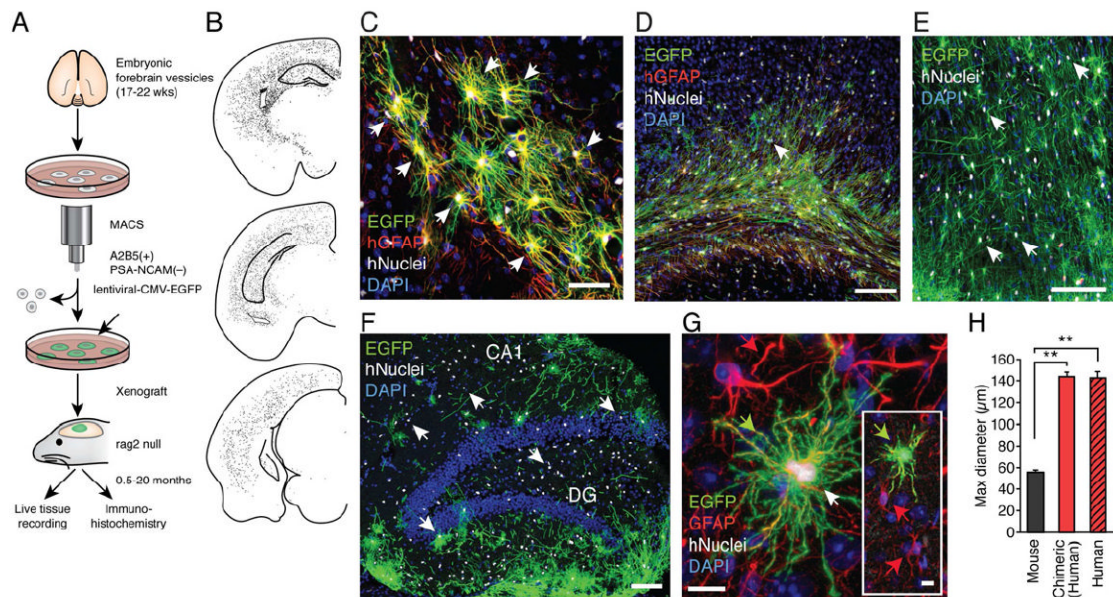
Figure 1. Human astrocytes replace host glia in mice engrafted with human glial progenitors
(**A**) Schematic outlining the procedure for magnetic cell sort-based isolation (MACS) of human glial progenitors, tagging with EGFP, and xenografting at P1. The chimeric mice brains were analyzed in 0.5-20 months old chimeric mice. (**B**) Representative dot map showing the distribution of human nuclear antigen (hNuclei)$^+$ cells in 3 coronal sections from a 10 months-old human chimeric mice. (**C**) The complex fine structure of human astrocytes in chimeric brain replicates the classical star-shaped appearance of human astrocytes labeled with hGFAP in situ. Most cells in the field are EGFP$^+$/hNuclei$^+$/hGFAP$^+$ (hGFAP, red). (**D**) At 5 months, EGFP$^+$ cells typically infiltrated corpus callosum and cortical layers V and VI. All EGFP$^+$ cells labeled with an antibody directed against human nuclear antigen (hNuclei) and most of the human cells were also labeled with an antibody directed against human GFAP (hGFAP, red). (**E**) At 11 months, many areas of cortex were infiltrated by evenly distributed EGFP+ /hNuclei$^+$ cells. (**F**) The hippocampus was also populated with EGFP+/hNuclei$^+$ cells in a 14 months old animal, with the highest density in the dentate. (**G**) Human EGFP$^+$/hNuclei$^+$/GFAP$^+$ cells (*green arrow*) were significantly larger than host murine astrocytes (*red arrow*). The anti-GFAP antibody cross-reacted with both human and mouse GFAP (*red*). Inset shows same field in lower magnification. (**H**) Histogram compares the diameter of mouse cortical astrocytes to human cortical astrocytes in situ (freshly resected surgical samples) and xenografted human astrocytes in cortex of chimeric mouse brain. The maximal diameter of mouse and human astrocytes (in situ and in chimeric mice) was determined in sections stained with an anti-GFAP antibody that labels both human and mouse GFAP. (n=50-65; **, *p*<0.01, Bonferroni t-test. (**B-F**): EGFP (*green*); hNuclei (*white* and *white arrow*); DAPI (*blue*).
Scale: 50 μm (**C**); 100 μm (**D-F**); and 10 μm (**G**). Data graphed as means ± SEM.
See also: Supplementary Figure S1.
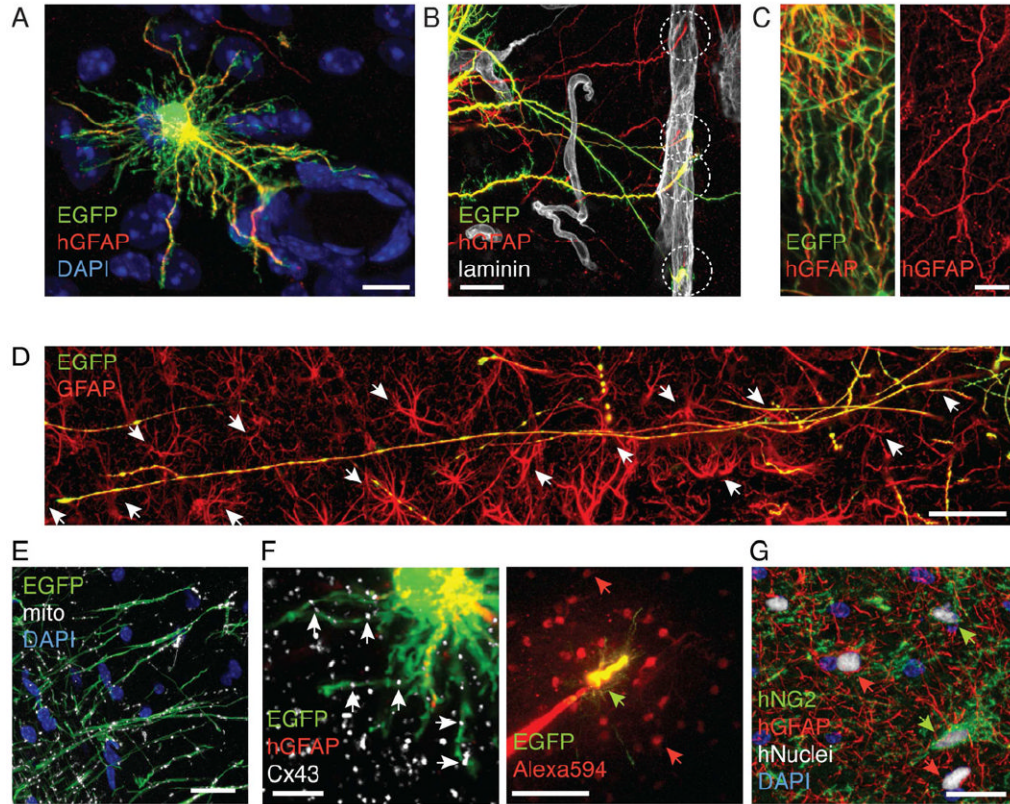
Figure 2. Human astrocytes retain hominid-specific morphology in chimeric mice

Human protoplasmic astrocytes matured in a cell-autonomous fashion in the chimeric mouse brain environment, retaining the long GFAP+, mitochondrial-enriched processes of native human astroglia. (**A**) An EGFP+/hGFAP+ astrocyte makes contact with the vasculature in a one month-old chimeric mice. (**B**) Long, unbranched EGFP+ and hGFAP+ astrocytic processes terminated (dashed circle) on the vasculature (laminin; *white*) 16 days after implantation. (**C**) The tortuous shape of EGFP+/hGFAP+ processes in chimeric brains replicate the appearance of GFAP+ processes of interlaminar astroglia in intact human tissue. (**D**) An example of EGFP+/GFAP+ process that spans > 600 μm and penetrates the domains of at least 14 host murine astrocytes (*white arrow*), (GFAP, *red*). (**E**) Long EGFP+ processes contain a large number of mitochondria (*white*) in an 11 month-old chimeric mouse. (**F**) An EGFP+/hGFAP+ human astrocyte express C×43 (*white*) gap junction plaques (*left panel*). An EGFP+ cell (*green arrow*) loaded with a small gap junction permeable tracer, Alexa 594 (MW 760) in a cortical slice (P15). Alexa 594 (red) diffused into multiple neighboring EGFP- cells (*red arrow*). (**G**) Co-existence of hGFAP+ (red)/hNuclei+ (*white*) cells (*red arrow*) and hNG2+(*green*)/hNuclei+ cells (*green arrow*) in the dentate of a 12 months old chimeric mouse. (**A-F**): EGFP (*green*); (**A-C**): hGFAP (*red*).

Scale bars: 10 μm (**A, C**); 20 μm (**B, E,G**); 50 μm (**D**) and (**F**) *right* panel; 5 μm (**F**) *left* panel.

See also: Supplementary Figure S2.
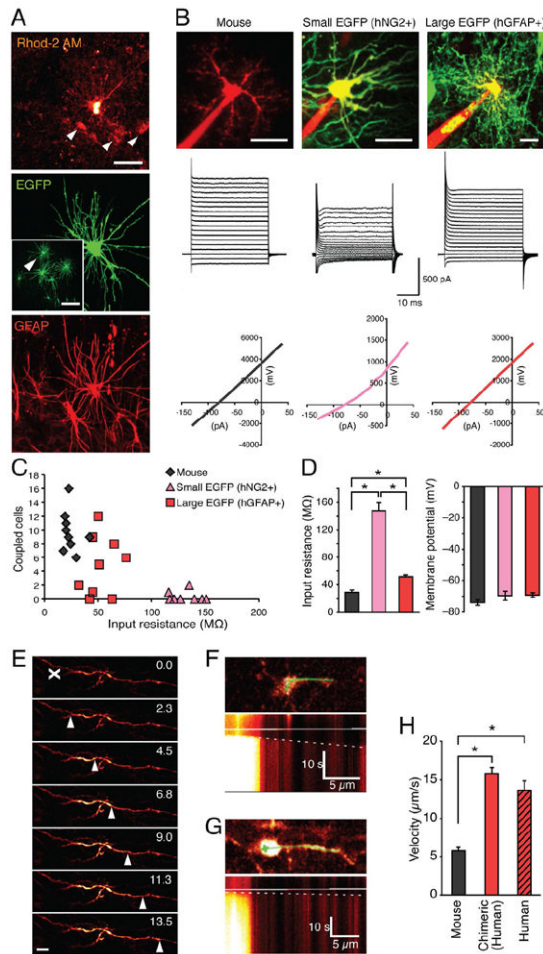
Figure 3. Functional properties indicate high-density host engraftment by both human glial progenitors and astrocytes

(**A**) Large and symmetric EGFP$^+$ cell (*green*) in an acute cortical slice prepared from a mouse engrafted with human glial progenitors 4 months earlier. *Inset*: lower magnification of the same field. The EGFP$^+$ cell was loaded filled with Rhod2 (red) by a path pipette. Rhod2 diffused into several neighboring EGFP- cells (white arrows, top panel). Cell identity was verified by immunolabeling against GFAP (red, below panel). Neighboring cells were GFAP+ and their shape characteristic of mouse astrocytes indicating that the human EGFP$^+$/GFAP$^+$ astrocytes was couple by functional gap junctions to host GFAP+ astrocytes. (**B**) I-V curves from host mouse astrocytes n=17; smaller, less complex EGFP$^+$ cells, presumably glial progenitor cells, n=14; and large and symmetric EGFP$^+$ cells, presumably astrocytes, n=37. (**C, D**) Comparison of the input resistance and gap junction coupled cells detected as number of neighboring cells labeled with Alexa 594. Mouse and large EGFP$^+$ cells (presumed human astrocytes) have a low input resistance, and are extensively coupled by gap junctions. In contrast, small EGFP$^+$ cells - presumed human GPCs - exhibited high input resistance and were not gap junction coupled. n=14-37, *; $p < 0.05$, Steel-Dwass test. (**E**) Photolysis of caged Ca^{2+} in an EGFP$^+$ astrocytic process. white "X" shows initiated point; white arrowhead shows Ca^{2+} propagation. (**F**) Top panel, line scan position across the length of a mouse astrocyte filled with NP-EGTA and rhod2. Below, line scan image of an intra-astrocytic Ca^{2+} wave initiated by photolysis of the cell body. White dashed line indicates the velocity of the intracellular Ca^{2+} wave. (**G**) Line scan image of a human astrocyte in a chimeric mouse (**H**) Comparison of velocities of intracellular Ca^{2+} waves in

host murine and engrafted human EGFP[+] astrocytes, and in human astrocytes in freshly resected surgical tissue. n=8-35, *; $p < 0.05$, Steel-Dwass test.

Scale: 30 µm (**A**); 100 µm (**A**) insert; 20 µm (**B**); 10 µm (**E**). Data graphed as means ± SEM.
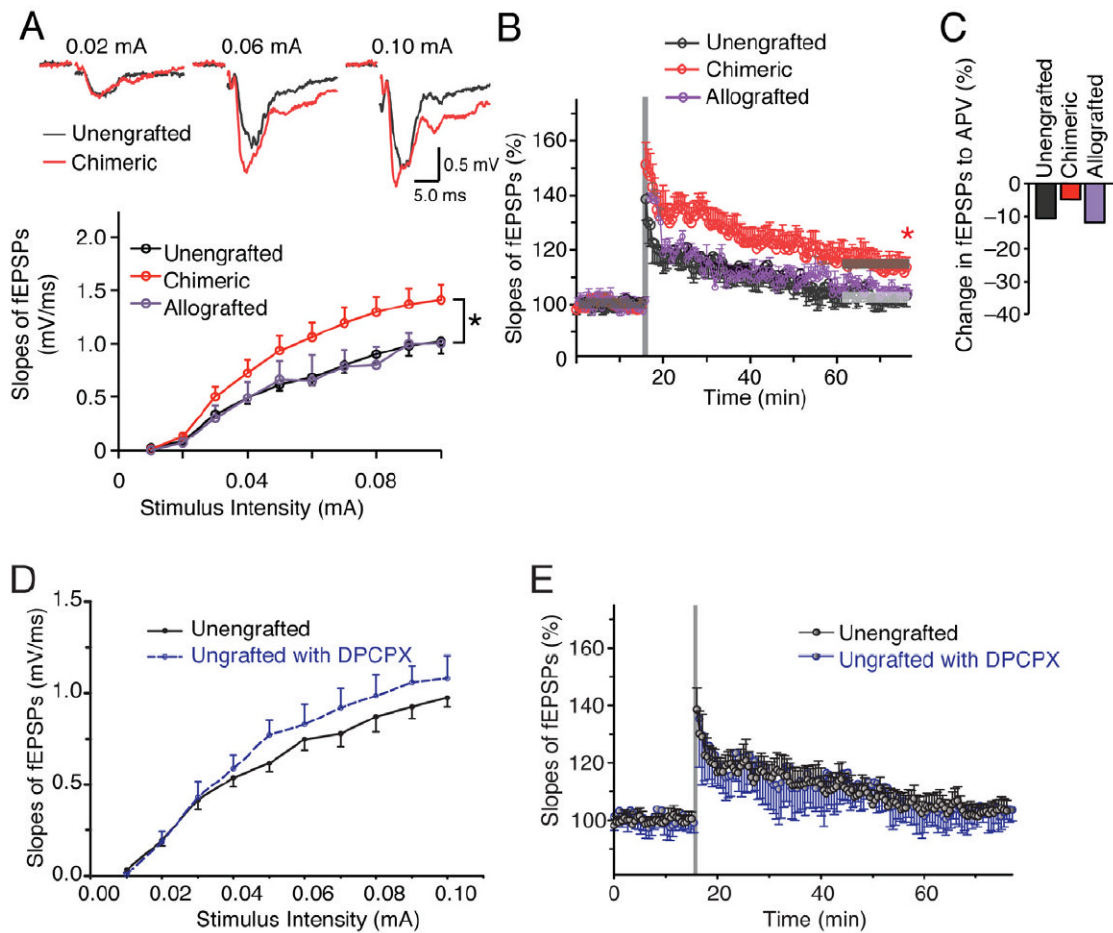
Figure 4. Strengthening of excitatory transmission and synaptic plasticity in murine brain by engrafting of human glial cells

(**A**) Comparison of field EPSPs (fEPSPs) in humanized chimeric mice and their unengrafted littermate and mouse GPC allografted controls. The slopes of fEPSP were significantly increased in human chimeric mice. (n=3-40; F=3.15, by two-way ANOVA with Bonferroni post hoc t test; *p<0.05) (**B**) Induction of LTP by 2-trains of high frequency stimulation (each train consisted of 100 pulses at 100 Hz, 30 s between bursts) in human chimeric mice, but not in unengrafted littermates and allografted mice. (n=7 mice each group); *, p < 0.05, t test compared between before and 60 min after the stimulation for each group (**C**) Relative decreased percentage of fEPSP by addition of NMDA receptor antagonist APV (50μM) in each group (n=15-27). (**D**) The adenosine A1 receptor antagonist, DPCPX failed to increase the fEPSP slope in unengrafted rag2 controls (100 nM DPCPX, n=8, p>0.05, Bonferroni test). (**E**) The adenosine A1 receptor antagonist, DPCPX did not decrease the threshold for induction of LTP in unengrafted controls; the fEPSP slope returned to 101.9 ± 3.6% by 60 min after HFS, similar to the rate of extinction in untreated slices (n = 8, t test).

Data graphed as means ± SEM.

See also: Supplementary Figure S3.
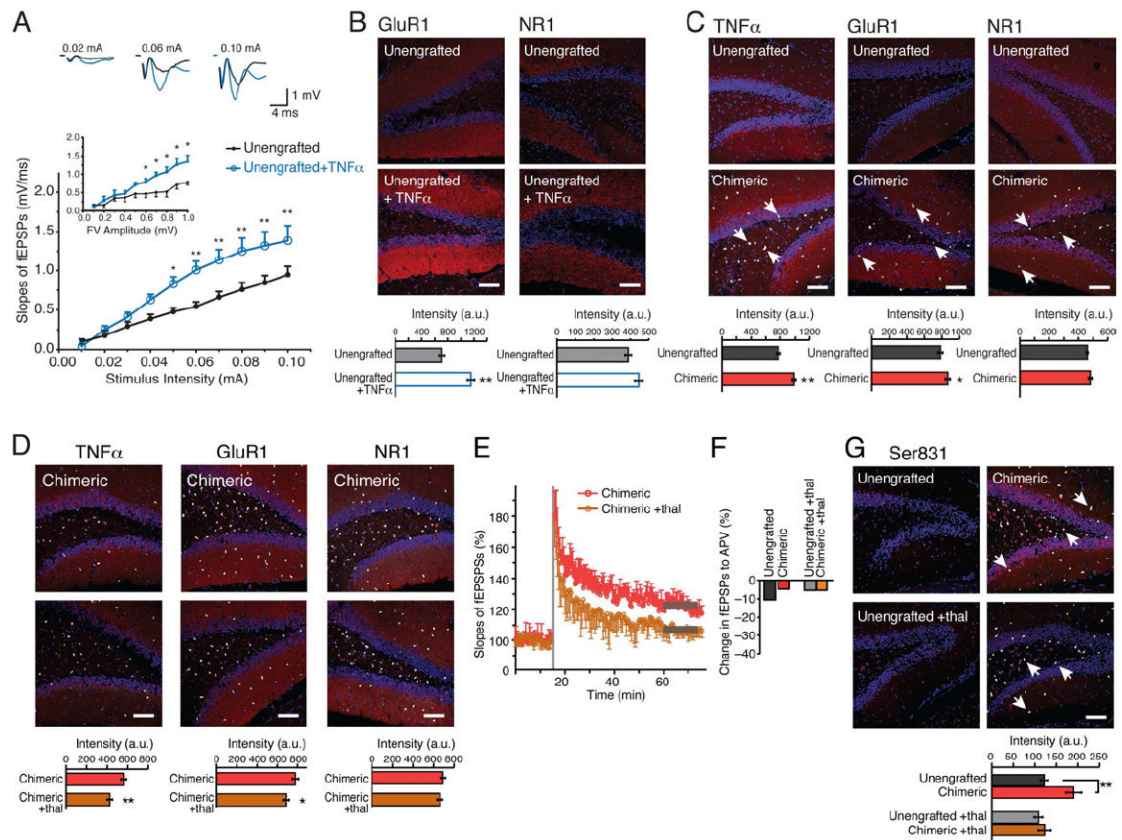
**Figure 5. Astrocytic TNFα contributes to LTP facilitation in chimeric mice, which is attenuated by thalidomide**

(**A**) Hippocampal slices prepared from littermate control rag1 mice exhibit a potentiation of fEPSP in response to TNFα (n=6, 12-16 months, *p<0.05; **: p<0.01; Bonferroni post hoc t test). *Inset:* fEPSP slopes plotted as a function of fiber volley amplitude. (**B**) Hippocampal slices exposed to TNFα (600 nM; 2-4 hrs.) exhibited an increase in the intensity of GluR1 subunit of AMPA receptors immunolabeling, but not of the NR1 subunit of NMDA receptors (n=5, 9-11months, **p<0.01, t-test). (**C**) Human chimeric mice exhibit higher intensity of immunolabeling against TNFα and GluR1, but not of NR1 (n=7, 7-20 months, *p<0.05, **p<0.01, t-test). (**D**) Thalidomide also decreased the immunolabeling of TNFα and GluR1, but not of NR1 in chimeric mice (n=6, 12-16 months, *; p<0.05, **; p<0.01, t-test). (**E**) The facilitation of LTP in chimeric mice was impaired by thalidomide (n=6, 12.6 ± 0.3 vs. 12.5 ± 0.5 months-old respectively, means ± SEM; p<0.05, t test). (**F**) Thalidomide did not change the contribution of NMDA receptor activation to fEPSP. Recordings of fEPSPs were obtained before and after addition of the NMDA receptor antagonist APV (50µM), and the difference calculated (n=4). (**G**) Phosphorylation of the Ser831 site of GluR1 was increased in chimeric mice compared with unengrafted littermate controls. Thalidomide attenuated the increase in phosphorylation of the Ser831 site of GluR1, but had no effect in unengrafted littermate controls, white arrows shows hNuclei^{+} cells. (n=6, 9-16 months, *p<0.05, t-test).

Scale bar: 100 µm (**B,C,D,G**). All data graphed as means ± SEM.

See also: Supplementary Figure S4.
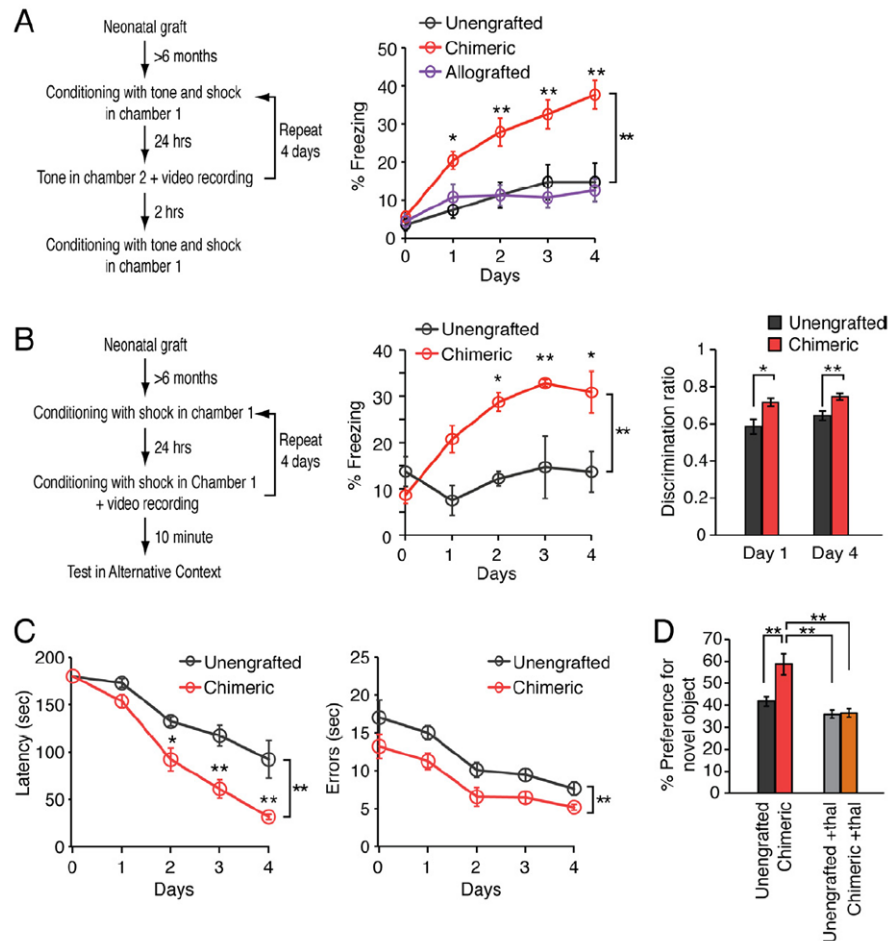
Figure 6. Humanized chimeric mice learn faster than controls

(**A**) Auditory fear conditioning assessed in a cohort of human chimeric, mouse chimeric, and unengrafted control rag1 mice. Chimeric mice exhibit prolonged freezing behavior in test chamber 2, during exposure to the tonal conditioned stimulus when compared to unengrafted mice and allografted mice (n = 5-20; *, p<0.05; **, p<0.01; two-way repeated measures ANOVA with Bonferroni test; means ± SEM). This difference persisted throughout all 4 days. (**B**) Contextual fear conditioning in human glial-chimeric mice and littermate controls. Freezing behavior was quantified for chimeric and unengrafted littermate controls during the two minutes of acclimatization period (n = 6; *, $p<0.05$; **, $p<0.01$; two-way repeated measures ANOVA with Bonferroni test). In addition the mean discrimination ratio for each day was obtained from freezing scores in the training chamber and the alternative chamber (freezing in training chamber/ total freezing time). Chimeric mice demonstrated significantly higher abilities to discriminate the chambers (n = 8-13; *, $p<0.05$; **, $p<0.01$; two-way repeated measures ANOVA with Bonferroni test). (**C**) Barnes maze testing in chimeric and unengrafted littermate controls. Chimeric mice demonstrated a significant learning advantage, as reflected in a shorter latency and fewer errors in solving the maze (n = 6; *, $p<0.05$; **, p<0.01; two-way repeated measures ANOVA with Bonferroni test). (**D**) Object-Location Memory Task (OLT) in chimeric mice and their unengrafted littermate controls demonstrated a learning advantage in chimeric mice via enhanced recognition of the novel displaced object. Thalidomide eliminated the learning advantage of chimeric mice

suggesting the learning enhancement was TNF-α mediated (n = 7; **, $p < 0.01$; one-way ANOVA with Bonferroni test).

All data plotted as means ± SEM.

See also: Supplementary Figure S5.